Two-dimensional angle-of-arrival estimation for uniform planar arrays with sensor position errors

Yih-Min Chen
Ju-Hong Lee
Chien-Chung Yeh

Indexing terms: Bearing estimation, Planar arrays, Direction finding

Abstract: The one-dimensional bearing estimation problem of linearly periodic arrays with sensor position errors has been tackled by the Toeplitz approximation method (TAM), iterative TAM, modified TAM, and iterative MTAM without calibrating the sensor positions. This paper extends these methods to the two-dimensional situation using a uniform planar array with sensor position errors to estimate the 2-D angle-of-arrivals (AOAs), azimuth and elevation angles of the emitting sources. Based on the block Toeplitz property and eigenstructure of the ideal covariance matrix observed by the unperturbed array, we extend the methods to alleviate the effect caused by the random perturbations in sensor position. The Music algorithm incorporating a 2-D AOA searching is applied for bearing estimation. Further, the 1-D processing approach presented earlier for solving the 2-D AOA estimation problem can also be applied to reduce the computational burden of 2-D AOA searching.

1 Introduction

Conventional approaches for solving the bearing estimation problem of arrays with the presence of sensor position errors generally calibrate sensor locations prior to performing bearing estimation [4–9]. In Reference 1, methods that need not calibrate the sensor positions have been proposed to tackle this problem when the sensor positions of a uniform linear array are randomly perturbed. These methods reconstruct a Toeplitz covariance matrix possessing the eigenstructure required for bearing estimation. The reconstructed covariance matrix is used as an estimate of the one observed by an unperturbed array, and Music algorithm is applied directly as though the array were unperturbed. The performance of these methods, depending on the number of the sensors and the variance of the sensor position errors, is discussed in Reference 1.

In this paper, we extend the methods of Reference 1, i.e. the Toeplitz approximation method (TAM), iterative TAM (ITAM), modified TAM (MTAM), and iterative MTAM (IMTAM), to the 2-D situation. The problem of estimating 2-D angles of arrival (AOA) of narrowband incoherent sources in the spatially white noise environment using a uniform planar array with the presence of sensor position errors is considered. In Section 2, we exploit two properties possessed by the covariance matrix of an unperturbed uniform planar array. The first is referred to as eigenstructure property, i.e. the property that the covariance matrix has as many significant eigenvalues which distinguish from noise power as the number of the emitting sources [2]. The other property concerned is that the covariance matrix exhibits block Toeplitz structure when the signal data received by the planar array is expressed in vector form. As to the covariance matrix of the randomly perturbed array, the eigenstructure property is preserved while the block Toeplitz structure is lost. Thus, for dealing with the 2-D situation, the procedure of TAM in References 1 and 10 is modified to restore the block Toeplitz structure of the covariance matrix. Similarly, the 2-D version of ITAM is formulated by incorporating the block Toeplitz procedure with the eigen-reconstruction procedure of Reference 1. MTAM and IMTAM are accommodated to the 2-D situation likewise. In addition to the modification of the matrix reconstruction procedure, the 1-D AOA searching performed in Reference 1 must be replaced by a 2-D AOA searching. To alleviate the computation load of the 2-D AOA searching, the approach presented in Reference 3 which consists of 1-D signal processing followed by a 2-D verification is also applied to the 2-D versions of TAM, ITAM, MTAM, and IMTAM.

2 Problem formulation and a review of 1-D methods

2.1 Problem formulation

Consider K far-field narrow-band and incoherent radiating sources observed by a uniform planar array of $M \times N$ sensors as shown in Fig. 1 with sensor position errors. With the (1, 1)th sensor as the origin and phase reference centre, the signal received by the (m, n)th sensor can be expressed by

$$v_{mn}(t) = \sum_{k=1}^{K} a_k(t) e^{j[\omega t + \kappa(x_k x_{mn} + \beta_k y_{mn})]} + n_{mn}(t) \quad (1)$$

where $a_k(t)$ denotes the signal amplitude of the kth source, κ is the wavenumber corresponding to the signal centre frequency ω, $n_{mn}(t)$ is the additive spatially white Gaussian noise with variance σ_n^2, $[x_{mn}, y_{mn}]$ is the sensor location, and $(\alpha_k, \beta_k) = (\cos \phi_k \cos \theta_k, \cos \phi_k \sin \theta_k)$ with θ_k and ϕ_k denoting the azimuth and elevation angles of the kth source, respectively. The location of the (m, n)th

Paper 9088F (E11, E15), first received 4th July 1990 and in revised form 25th June 1992

Yih-Min Chen was with, and Ju-Hong Lee and Chien-Chung Yeh are with the Department of Electrical Engineering, National Taiwan University, Taipei, Taiwan, Republic of China

Yih-Min Chen is now with the Department of Electrical Engineering, Yuan-Ze Institute of Technology, Chung-Li, Taiwan, Republic of China

sensor is given by

$$[x_{mn}, y_{mn}] = [(m-1)\,d_x, (n-1)\,d_y] + [\Delta x_{mn}, \Delta y_{mn}] \quad (2)$$

where d_x and d_y denote the interelement spacings in the row and column directions, respectively, and Δx_{mn} and

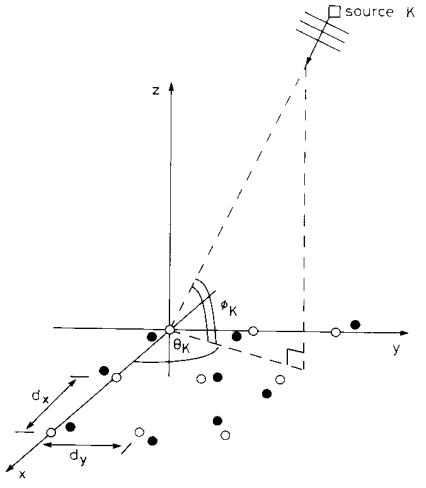

Fig. 1 *Geometrical illustration of 2-D bearing estimation problem using 3 × 3 uniform planar array with sensor position errors*

θ_k azimuth; ϕ_k elevation
● actual sensor location
○ nominal location

Δy_{mn} are the position perturbations with same variance σ_e^2. Then the covariance matrix of the received signals of the sensors is expressed as

$$\boldsymbol{R} = E[\boldsymbol{v}(t)\boldsymbol{v}\dagger(t)] = \sum_{k=1}^{K} a_k^2\, \boldsymbol{P}^k \hat{\boldsymbol{s}}_k \hat{\boldsymbol{s}}_k^{\dagger} (\boldsymbol{P}^k)^{\dagger} + \sigma_n^2 \boldsymbol{I} \quad (3)$$

where

$$\boldsymbol{v}(t) = [\boldsymbol{v}_1^T(t), \boldsymbol{v}_2^T(t), \ldots, \boldsymbol{v}_N^T(t)]^T \quad (4)$$

$$\boldsymbol{v}_n(t) = [v_{1n}(t), v_{2n}(t), \ldots, v_{Mn}(t)]^T, \quad n = 1, 2, \ldots, N \quad (5)$$

$$a_k^2 = E[|a_k(t)|^2] \quad (6)$$

$$\boldsymbol{P}^k = \text{diag}\,(\boldsymbol{P}_1^k, \boldsymbol{P}_2^k, \ldots, \boldsymbol{P}_N^k) \quad (7)$$

$$\boldsymbol{P}_n^k = \text{diag}\,(e^{j\kappa(\alpha_k \Delta x_{1n} + \beta_k \Delta y_{1n})}, e^{j\kappa(\alpha_k \Delta x_{2n} + \beta_k \Delta y_{2n})}, \ldots, e^{j\kappa(\alpha_k \Delta x_{Mn} + \beta_k \Delta y_{Mn})}) \quad (8)$$

$$\hat{\boldsymbol{s}}_k = [\hat{\boldsymbol{s}}_k^{(r)}, e^{j\kappa\beta_k d_y}\hat{\boldsymbol{s}}_k^{(r)}, \ldots, e^{j\kappa\beta_k(N-1)d_y}\hat{\boldsymbol{s}}_k^{(r)}]^T \quad (9)$$

$$\hat{\boldsymbol{s}}_k^{(r)} = [1, e^{j\kappa\alpha_k d_x}, \ldots, e^{j\kappa\alpha_k(M-1)d_x}] \quad (10)$$

$\boldsymbol{I}$ is the identity matrix, T and † denote the transpose and complex conjugate transpose operations, respectively. The $\boldsymbol{P}^k$ in eqn. 7 represents the effect of sensor position errors. Eqn. 8 shows that this effect depends on the source bearing and $[\Delta x_{mn}, \Delta y_{mn}]$, $m = 1, 2, \ldots, M$, $n = 1, 2, \ldots, N$. In eqn. 3, $\hat{\boldsymbol{s}}_k$ indicates the direction vector model of a far-field source when the array is unperturbed, i.e. $[\Delta x_{mn}, \Delta y_{mn}] = [0, 0]$ for all m and n. From eqns. 3–10, it is noted that when the array is unperturbed, the covariance matrix, referred to as $\hat{\boldsymbol{R}}$, exhibits a block Toeplitz structure and has K significant eigenvalues greater than σ_n^2 since

$$\hat{\boldsymbol{R}} = \sum_{k=1}^{K} a_k^2\, \hat{\boldsymbol{s}}_k \hat{\boldsymbol{s}}_k^{\dagger} + \sigma_n^2 \boldsymbol{I} = [\hat{\boldsymbol{R}}_{ij}]_{N \times N} \quad (11)$$

where

$$\hat{\boldsymbol{R}}_{ij} = \hat{\boldsymbol{R}}_{i-j} = \sum_{k=1}^{K} a_k^2\, e^{j\kappa\beta(j-i)d_y}\hat{\boldsymbol{s}}_k^{(r)}(\hat{\boldsymbol{s}}_k^{(r)})^{\dagger} + \delta[i-j]\sigma_n^2 \boldsymbol{I} \quad (12)$$

denotes the $M \times M$ cross-covariance matrix of the ith and jth row subarrays, which has Toeplitz structure, and $\delta[k]$ is the discrete impulse function. As to the covariance matrix $\boldsymbol{R}$ of the perturbed array, the block Toeplitz structure is lost and its signal subspace is spanned by $\boldsymbol{P}^k\hat{\boldsymbol{s}}_k$, $k = 1, 2, \ldots, K$, instead of $\hat{\boldsymbol{s}}_k$. Therefore, direct application of bearing estimation algorithms based on $\boldsymbol{R}$ using the direction vector model $\hat{\boldsymbol{s}}_k$ will degrade the array performance. Generally, this problem is solved by calibrating sensor position prior to performing bearing estimation in the literature.

2.2 Review of 1-D methods

In the 1-D case, the problem is formulated as that given by eqns. 2–12 with $N = 1$ and $\phi_k = 0°$, $k = 1, 2, \ldots, K$. Instead of calibrating the perturbed sensor positions, the methods of Reference 1 try to reduce the effect of the sensor position perturbations by estimating $\hat{\boldsymbol{R}}$ using certain structure reconstruction procedures. Then, bearing estimation algorithms are applied based on the estimate of $\hat{\boldsymbol{R}}$, denoted by $\bar{\boldsymbol{R}}$, using the original direction vector model $\hat{\boldsymbol{s}}_k$. TAM, ITAM, MTAM, and IMTAM, having different estimates of $\hat{\boldsymbol{R}}$, are summarised as follows:

2.2.1 TAM: This method estimates $\hat{\boldsymbol{R}}$ by the following Toeplitz structure reconstruction formula:

$$\bar{\boldsymbol{R}}_T = T[\boldsymbol{R}] = [(\bar{r}_T)_{ij}] = [\bar{r}_T(i-j)] \quad (13)$$

where

$$\bar{r}_T(-m) = \frac{1}{M-m}\sum_{i=1}^{M-m} r_{i(i+m)}, \quad 0 \leqslant m < M$$

$$\bar{r}_T(m) = \bar{r}_T^{\dagger}(-m) \quad (14)$$

and $r_{i(i+m)}$ is the $(i, i+m)$th entry of $\boldsymbol{R}$. It is noted that $\bar{\boldsymbol{R}}_T$ is the solution of the following problem [1]

$$\min_{\boldsymbol{R}_T \in \boldsymbol{S}_T} \|\bar{\boldsymbol{R}}_T - \boldsymbol{R}\| \quad (15)$$

where $\boldsymbol{S}_T$ is the set of Toeplitz matrices, and '$\|\boldsymbol{A}\|$' denotes the Frobenius norm of the matrix $\boldsymbol{A}$ [11].

2.2.2 ITAM: The ITAM method iteratively performs the Toeplitz structure reconstruction operation of the TAM and an eigenstructure reconstruction operation to obtain the estimate $\bar{\boldsymbol{R}}_{IT}$. The procedure is summarised as

(*a*) $\bar{\boldsymbol{R}}_E^{(0)} = \boldsymbol{R}$ and $i = 0$,
(*b*) $\bar{\boldsymbol{R}}_T^{(i+1)} = T[\bar{\boldsymbol{R}}_E^{(i)}]$,
(*c*) $\bar{\boldsymbol{R}}_E^{(i+1)} = \bar{E}[\bar{\boldsymbol{R}}_T^{(i+1)}]$,
(*d*) if $\|\bar{\boldsymbol{R}}_E^{(i+1)} - \bar{\boldsymbol{R}}_T^{(i+1)}\| > \varepsilon$, then $i = i + 1$ and repeat (*b*)–(*d*),
(*e*) $\bar{\boldsymbol{R}}_{IT} = \bar{\boldsymbol{R}}_E^{(i+1)}$.

where the eigenstructure reconstruction operation $\bar{E}[\ ]$ is formulated as [12]

$$\bar{\boldsymbol{R}}_E = \bar{E}[\boldsymbol{R}] = \sum_{k=1}^{K} \lambda_k \boldsymbol{e}_k \boldsymbol{e}_k^\dagger + \lambda_{av} \sum_{i=K+1}^{MN} \boldsymbol{e}_i \boldsymbol{e}_i^\dagger \quad (16)$$

where $\lambda_1 \geqslant \lambda_2 \geqslant \cdots \geqslant \lambda_{MN}$ and $\boldsymbol{e}_i$, $i = 1, 2, \ldots, MN$ are the eigenvalues and the corresponding eigenvectors of $\boldsymbol{R}$, respectively, and λ_{av} is the average of $\lambda_{K+1}, \lambda_{K+2}, \ldots, \lambda_{MN}$.

2.2.3 MTAM: The MTAM method uses a modified Toeplitz structure reconstruction operation which is given by

$$\bar{\boldsymbol{R}}_{MT} = MT[\boldsymbol{R}] = [(\bar{r}_{MT})_{ij}] = [\bar{r}_{MT}(i-j)] \quad (17)$$

$$\bar{r}_{MT}(-m) = \left(\frac{1}{M-m} \sum_{i=1}^{M-m} |r_{i(i+m)}|\right) \times \exp\left[j \arg\left(\frac{1}{M-m} \sum_{i=1}^{M-m} r_{i(i+m)}\right)\right]$$

$$\bar{r}_{MT}(m) = \bar{r}_{MT}^{\dagger}(-m), \quad 0 \leqslant m < M \quad (18)$$

where arg (x) represents the argument of the complex scalar x.

2.2.4 IMTAM: This method uses the same procedure as that of the ITAM method except the Toeplitz structure reconstruction operation is replaced by that of the MTAM method. The estimate is represented by $\bar{\boldsymbol{R}}_{IM}$. The convergence of the iterative methods is ensured since all the matrix operations are norm-reduced and constant trace operations.

3 2-D versions of TAM, ITAM, MTAM, and IMTAM

In this Section, we present the 2-D versions of the methods proposed in Reference 1 for the 2-D AOA estimation problem. Analogous to the 1-D case, the block Toeplitz structure and the eigenstructure associated with $\bar{\boldsymbol{R}}$ are used to obtain the estimates of $\bar{\boldsymbol{R}}$ from the observed covariance matrix $\boldsymbol{R}$.

3.1 2-D TAM

The 2-D TAM considers the restoration of block Toeplitz structure. The problem can be formulated as

$$\min_{\boldsymbol{R}_{BT} \in \boldsymbol{S}_{BT}} \|\boldsymbol{R}_{BT} - \boldsymbol{R}\| \quad (19)$$

where $\boldsymbol{S}_{BT}$ is the set of block Toepliz matrices. To formulate the solution for eqn. 19, the observed covariance matrix $\boldsymbol{R}$ is first rewritten as

$$\boldsymbol{R} = \begin{bmatrix} \boldsymbol{R}_{11} & \boldsymbol{R}_{12} & \boldsymbol{R}_{13} & \cdots & \boldsymbol{R}_{1N} \\ \boldsymbol{R}_{21} & \boldsymbol{R}_{22} & \boldsymbol{R}_{23} & \cdots & \vdots \\ \vdots & & \ddots & & \\ \boldsymbol{R}_{N1} & \cdots & & & \boldsymbol{R}_{NN} \end{bmatrix} \quad (20)$$

where $\boldsymbol{R}_{ij}$ is the $M \times M$ cross-covariance of the ith and jth row subarrays. The estimate of $\hat{\boldsymbol{R}}$ obtained by TAM is then

$$\bar{\boldsymbol{R}}_{BT} = BT[\boldsymbol{R}] = \begin{bmatrix} \bar{\boldsymbol{R}}_0 & \bar{\boldsymbol{R}}_{-1} & \bar{\boldsymbol{R}}_{-2} & \cdots & \bar{\boldsymbol{R}}_{(1-N)} \\ \bar{\boldsymbol{R}}_{-1}^{\dagger} & \bar{\boldsymbol{R}}_0 & \bar{\boldsymbol{R}}_{-1} & \cdots & \vdots \\ \vdots & & \ddots & & \\ \bar{\boldsymbol{R}}_{(1-N)}^{\dagger} & \cdots & & & \bar{\boldsymbol{R}}_0 \end{bmatrix} \quad (21)$$

where

$$\bar{\boldsymbol{R}}_{-n} = \frac{1}{N-n} \sum_{i=1}^{N-n} \mathrm{T}[\boldsymbol{R}_{i(i+n)}], \quad n = 0, 1, \ldots, N-1 \quad (22)$$

are all Toeplitz matrices with size $M \times M$ and T[ ] denotes the Toeplisation operation given in eqn. 13. Consequently, estimating 2-D AOAs using the 2-D TAM is summarised as follows: First, compute $\bar{\boldsymbol{R}}_{BT}$ from $\boldsymbol{R}$ by eqn. 21 and then apply Music based on $\bar{\boldsymbol{R}}_{BT}$ with the incorporation of 2-D AOA searching.

3.2 2-D ITAM

The extension of ITAM to the 2-D case is straightforward by replacing the Toeplitzation procedure with the above block Toeplitzation procedure during the iteration process for restoring the required eigenstructure and block Toeplitz structure.

3.3 2-D MTAM

The MTAM can be extended similarly by modifying the block Toeplization procedure as follows. The $\bar{\boldsymbol{R}}_{-n}$ of eqn. 22 is replaced by

$$\bar{\boldsymbol{R}}_{-n} = \mathrm{MTM}\{\mathrm{MT}[\boldsymbol{R}_{1(1+n)}], \mathrm{MT}[\boldsymbol{R}_{2(2+n)}], \ldots, \mathrm{MT}[\boldsymbol{R}_{(N-n)N}]\} \quad (23)$$

where MT[ ] denotes the modified Toeplization operation of eqn. 17 and the operation MTM{ } is given by

$$\tilde{\boldsymbol{R}} = \mathrm{MTM}\{\boldsymbol{R}^1, \boldsymbol{R}^2, \ldots, \boldsymbol{R}^P\} = \begin{bmatrix} \tilde{r}_{11} & \tilde{r}_{12} & \tilde{r}_{13} & \cdots & \tilde{r}_{1M} \\ \tilde{r}_{21} & \tilde{r}_{22} & \tilde{r}_{23} & & \\ \vdots & & \ddots & & \vdots \\ \tilde{r}_{M1} & \cdots & & & \tilde{r}_{MM} \end{bmatrix} \quad (24)$$

$$\tilde{r}_{ij} = \left(\frac{1}{P} \sum_{k=1}^{P} |r_{ij}^k|\right) \exp\left[j \arg\left(\sum_{k=1}^{P} r_{ij}^k\right)\right] \quad (25)$$

In eqn. 25, r_{ij}^k is the (i, j)th entry of $\boldsymbol{R}^k$. The resultant block Toeplitz matrix is denoted as $\bar{\boldsymbol{R}}_{MBT} = \mathrm{MBT}[\boldsymbol{R}]$, where MBT[ ] represents the modified block Toeplitzation operation.

3.4 2-D IMTAM

Again, the extension of the IMTAM method to the 2-D case is straightforward by replacing the modified Toeplitzation procedure with the modified block Toeplitzation procedure during the iteration process.

The procedures of the 2-D versions of TAM, ITAM, MTAM, and IMTAM are summarised in Fig. 2. The convergence of ITAM and IMTAM is again ensured since all the matrix operations are norm-reduced and constant trace operations.

3.5 1-D processing approach

To alleviate the computation load of 2-D AOA searching, the 1-D processing approach described in Reference 3 can be employed. Doing so requires the estimates of the $\bar{\boldsymbol{R}}_r$ and $\bar{\boldsymbol{R}}_c$ the covariance matrices associated with the unperturbed row and column subarrays, respectively. The $\bar{\boldsymbol{R}}_r$ and $\bar{\boldsymbol{R}}_c$ can be obtained from the reconstructed covariance matrices. Hence, they are Toeplitz and possess the

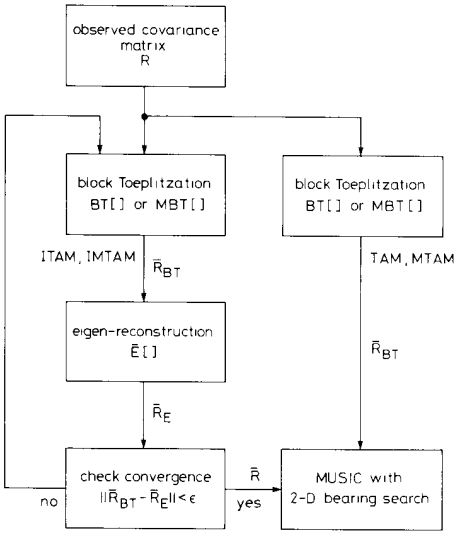

Fig. 2 *Flow diagram of 2-D versions of TAM, MTAM, ITAM, and IMTAM*

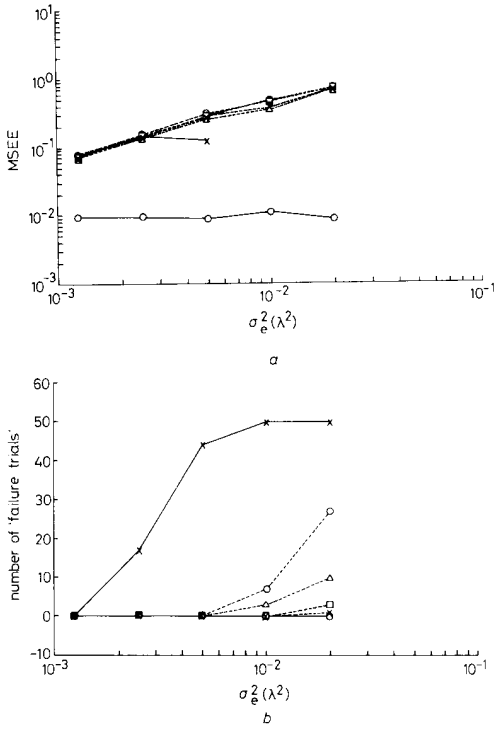

Fig. 3 *Statistical performance of proposed methods for cases of* $(\theta_1, \phi_1) = (21°, 40°)$, $(\theta_2, \phi_2) = (25°, 44°)$, *of SNR = 3 dB and* $\sigma_e^2 = 0.00125\lambda^2, 0.0025\lambda^2, 0.005\lambda^2, 0.01\lambda^2, 0.02\lambda^2$

a mean squared estimation error
b number of 'failure trials'
×——× Music without calibration
○——○ Music with calibration
○- - -○ TAM
□- - -□ ITAM
△- - -△ MTAM
×- - -× IMTAM

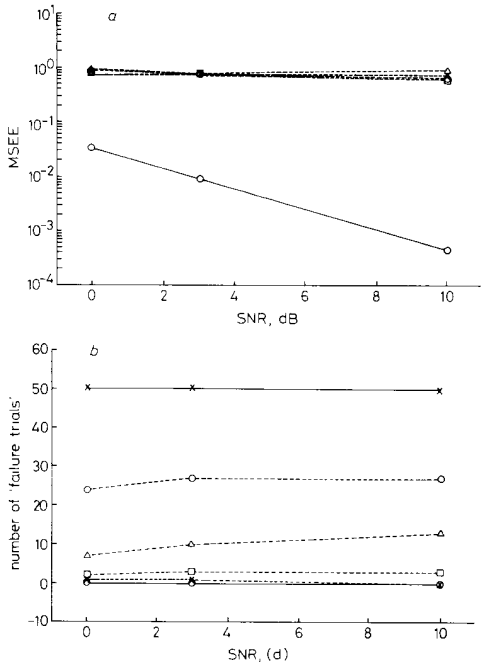

Fig. 4 *Statistical performance of proposed methods for cases* $(\theta_1, \phi_1) = (21°, 40°)$, $(\theta_2, \phi_2) = (25°, 44°)$, *of* $\sigma_e^2 = 0.02\lambda^2$ *and SNR = 0, 3, 10 dB*

a mean squared estimation error
b number of 'failure trials'
×——× Music without calibration
○——○ Music with calibration
○- - -○ TAM
□- - -□ ITAM
△- - -△ MTAM
×- - -× IMTAM

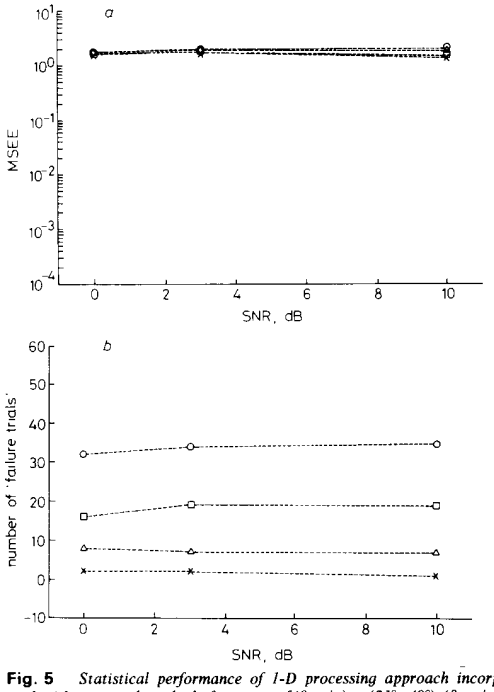

Fig. 5 *Statistical performance of 1-D processing approach incorporated with proposed methods for cases of* $(\theta_1, \phi_1) = (21°, 40°)$, $(\theta_2, \phi_2) = (25°, 44°)$, $\sigma_e^2 = 0.02\lambda^2$, *and SNR = 0, 3, 10 dB*

a mean squared estimation error
b number of 'failure trials'
○- - -○ TAM-1D
□- - -□ ITAM-1D
△- - -△ MTAM-1D
×- - -× IMTAM-1D

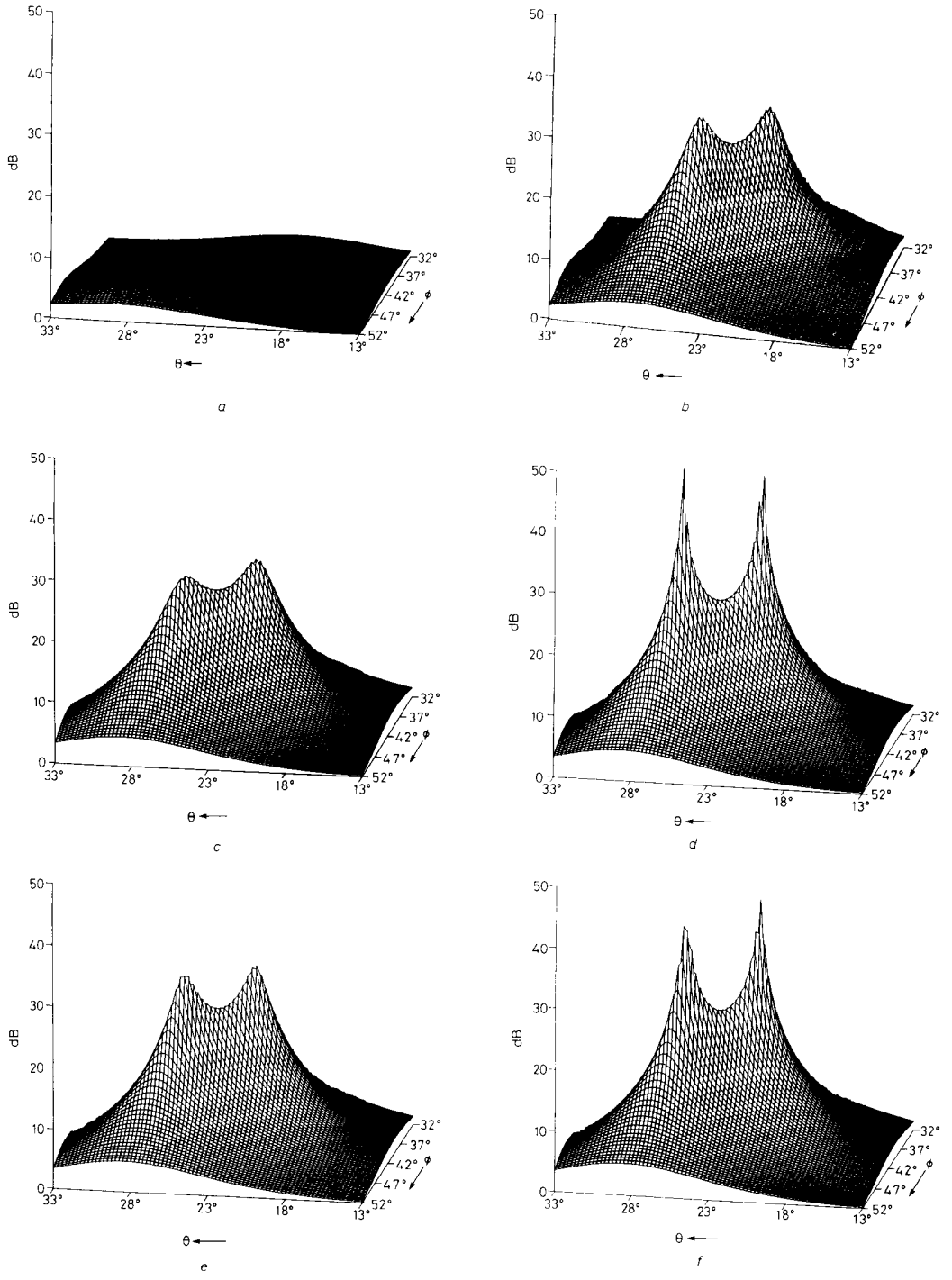

Fig. 6 *2-D bearing spectra of proposed methods in selected simulation for case of* $(\theta_1, \phi_1) = (21°, 40°)$, $(\theta_2, \phi_2) = (25°, 44°)$, $SNR = 3$ *dB and* $\sigma_e^2 = 0.02\lambda^2$

a Music without calibration
b Music with precise calibration
c TAM
d ITAM
e MTAM
f IMTAM

desired eigenstructure. The estimate $\bar{R}_r$ with size $M \times M$ is given by

$$\bar{R}_r = \bar{R}_0, \tag{26}$$

and $\bar{R}_c$ with size $N \times N$ is

$$\bar{R}_c = \begin{bmatrix} \bar{r}^c_{11} & \bar{r}^c_{12} & \bar{r}^c_{13} & \cdots & \bar{r}^c_{1N} \\ \bar{r}^c_{21} & \bar{r}^c_{22} & \bar{r}^c_{23} & & \\ \vdots & & \ddots & & \vdots \\ \bar{r}^c_{N1} & & \cdots & & \bar{r}^c_{NN} \end{bmatrix} \tag{27}$$

where

$\bar{r}^c_{ij}$ is the (1, 1)th entry of $\bar{R}_{(i-j)}$ in eqn. 6. (28)

Based on $\bar{R}_r$, we can apply Music with the 1-D searching to estimate the values of α_k, $k = 1, 2, \ldots, K$. Similarly, the estimates of β_p, $p = 1, 2, \ldots, K$, can be obtained from $\bar{R}_c$. Finally, the 2-D verification presented in Reference 3 must be performed to obtain the estimates of the 2-D AOAs of the emitting sources.

4 Simulation results

We used a uniform planar array of 10×10 sensors with half-wavelength interelement spacing in both row and column directions for simulation. The sensor position perturbations $[\Delta x_{ij}, \Delta y_{ij}]$, $i, j = 1, 2, \ldots, 10$, were obtained by Gaussian random number generator, all with same variance σ_e^2. Two equally powered incoherent emitting sources with 2-D bearings $(\theta_1, \phi_1) = (21°, 40°)$ and $(\theta_2, \phi_2) = (25°, 44°)$, respectively, were observed by the array. 500 snapshots were taken to compute the covariance matrix $\boldsymbol{R}$. Fig. 3 shows the statistical performance of the 2-D versions of TAM, ITAM, MTAM and IMTAM for the cases that $\sigma_e^2 = 0.00125\lambda^2$, $0.0025\lambda^2$, $0.005\lambda^2$, $0.01\lambda^2$, and $0.02\lambda^2$ with signal-to-noise ratio (SNR) of 3 dB. The statistical results of the mean squared estimation error and the number of 'failure trails' were obtained by Monte Carlo simulation with 50 independent trials. The mean squared estimation error is computed by

$$\frac{1}{L}\sum_{i=1}^{L} \frac{(\hat{\theta}_1^{(i)} - \theta_1)^2 + (\hat{\phi}_1^{(i)} - \phi_1)^2 + (\hat{\theta}_2^{(i)} - \theta_2)^2 + (\hat{\phi}_2^{(i)} - \phi_2)^2}{4} \tag{29}$$

where $(\hat{\theta}_k^{(i)}, \hat{\phi}_k^{(i)})$, $k = 1, 2$, denote the estimates in the ith 'successful' trial and L is the number of 'successful' trials. Trials are designated as 'failure' when the two close sources cannot be resolved. Fig. 4 shows the results of the cases that SNR = 0, 3 and 10 dB with σ_e^2 fixed at $0.02\lambda^2$. The results of 1-D processing approach incorporated with the 2-D versions of TAM, ITAM, MTAM and IMTAM, denoted as the TAM-1D, ITAM-1D, MTAM-1D, and IMTAM-1D, respectively, are shown in Fig. 5 for the same cases. The simulation results of Music with no calibration and precise calibration are also included for comparison. The proposed methods have similar performance tendency as in the 1-D situation [1]. These results also show that although 1-D processing approaches have advantage in saving computation load, their performances are sacrificed. Fig. 6 shows the 2-D bearing spectra using Music with no calibration and precise calibration, and the proposed methods in a selected simulation for the case of SNR = 3 dB and $\sigma_e^2 = 0.02\lambda^2$.

5 Conclusions

The methods in Reference 1 dealing with the problem of estimating source bearings using a uniform linear array with sensor position errors were extended to solve the similar problem for a uniform planar array. With the estimation of the ideal covariance matrix for the unperturbed array, which is based on the block Toeplitz structure and eigenstructure reconstruction approach, the problem was tackled without calibrating the sensor positions. The extended methods have similar performance tendency as the original 1-D methods. These methods have the advantage of simplicity over the conventional calibration approaches.

6 References

1 CHEN, Y.-M., LEE, J.-H., YEH, C.-C., and MAR, J.: 'Bearing estimation without calibration for randomly perturbed arrays', *IEEE Trans.*, 1991, **SP-39**, pp. 194–197

2 SCHMIDT, R.: 'A signal subspace approach to multiple emitter location and signal parameter estimation'. PhD dissertation, Stanford University, Stanford, CA, USA, 1981

3 YEH, C.-C., LEE, J.-H., and CHEN, Y.-M.: 'Estimating two-dimensional angles of arrival in coherent source environment', *IEEE Trans.*, 1989, **ASSP-37**, pp. 153–155

4 SEYMOUR, L.P.H.K., COWAN, C.F.N., and GRANT, P.M.: 'Bearing estimation in the presence of sensor position errors'. Proceedings of ICASSP, Dallas, USA, 1987, pp. 2264–2267

5 LO, J.T., and MARPLE, S.L.: 'Eigenstructure methods for array sensor location'. Proceedings of ICASSP, Dallas, USA, 1987, pp. 2260–2263

6 ROCKAH, Y., and SCHULTHEISS, P.M.: 'Source location with two-dimensional array subject to uncertainty in sensor location'. Proceedings of ICASSP, Tokyo, Japan, 1986, pp. 1885–1888

7 ROCKAH, Y., and SCHULTHEISS, P.M.: 'Array shape calibration using sources in unknown locations. Part I: far-field sources', *IEEE Trans.*, 1987, **ASSP-35**, pp. 286–299

8 ROCKAH, Y., and SCHULTHEISS, P.M.: 'Array shape calibration using sources in unknown locations. Part II: near-field sources', *IEEE Trans.*, 1987, **ASSP-35**, pp. 724–735

9 WEISS, A.J., and FRIEDLANDER, B.: 'Array shape calibration using sources in unknown locations — a maximum likelihood approach'. Proceedings of ICASSP, New York, USA, 1988, pp. 2670–2673

10 KUNG, S.Y., LO, C.K., and FOKA, R.: 'A Toeplitz approximation approach to coherent source direction finding'. Proceedings of ICASSP, Tokyo, Japan, 1986, pp. 193–196

11 CADZOW, J.A.: 'Signal enhancement — A composite property mapping algorithm', *IEEE Trans.*, 1988, **ASSP-36**, pp. 49–62

12 WILKES, D.M., and HAYES, M.H.: 'Iterated Toeplitz approximation of covariance matrices'. Proceedings ICASSP, New York, USA, 1988, pp. 1663–1666